MOLECULAR AND CELLULAR BIOLOGY, Oct. 2003, p. 7152–7162 Vol. 23, No. 20
0270-7306/03/$08.00+0 DOI: 10.1128/MCB.23.20.7152–7162.2003

Processing of Double-Strand Breaks Is Involved in the Precise Excision of *Paramecium* Internal Eliminated Sequences

Ariane Gratias and Mireille Bétermier*

Laboratoire de Génétique Moléculaire, CNRS UMR 8541, Ecole Normale Supérieure, 75005 Paris, France

Received 17 April 2003/Returned for modification 26 May 2003/Accepted 21 July 2003

In ciliates, the development of the somatic macronucleus involves the programmed excision of thousands of internal eliminated sequences (IES) scattered throughout the germ line genome. Previous work with *Tetrahymena thermophila* has suggested that excision is initiated by a staggered double-strand break (DSB) at one IES end. Nucleophilic attack of the other end by the 3′OH group carried by the firstly broken chromosome end leads to macronuclear junction closure. In this study, we mapped the 3′OH and 5′PO_4 groups that are developmentally released at *Paramecium* IES boundaries, which are marked by two conserved TA dinucleotides, one of which remains in the macronuclear genome after excision. We show that initiating DSBs at both ends generate 4-base 5′ overhangs centered on the TA. Based on the observed processing of the 5′-terminal residue of each overhang, we present a new model for the precise closure of macronuclear chromosomes in *Paramecium tetraurelia*, different from that previously proposed for *Tetrahymena*. In our model, macronucleus-destined broken ends are aligned through the partial pairing of their 5′-nTAn-3′ extensions and joined after trimming of the 5′ flaps.

Recombination processes involving the cutting and rejoining of DNA molecules have been found in a wide range of organisms, and two types of molecular mechanisms have been documented (reviewed in reference 5): conservative site-specific recombination, leading to the deletion/insertion or inversion of DNA sequences, involves the transient formation of covalent protein-DNA intermediates, while other reactions, such as the transposition of most class II transposons, generate DNA intermediates. Ciliates provide attractive models for the study of programmed DNA rearrangements and their regulation, because their entire genome is remodeled at each sexual cycle (reviewed in references 13 and 34). In addition, these events can be induced experimentally following cell starvation (see, e.g., reference 30 for the *Paramecium aurelia* group of species). The molecular mechanisms involved in the rearrangements, however, remain largely unknown.

A characteristic feature of ciliates is the presence, within the same cytoplasm, of two structurally and functionally different nuclei. The highly polyploid macronucleus, also called the somatic nucleus, controls the cell phenotype but is lost at each sexual reproduction event. In contrast, the germ line diploid micronucleus undergoes meiosis and transmits its genome to the zygotic nucleus of the next sexual generation. Following two mitotic divisions of the zygotic nucleus, two nuclei become the new micronuclei. The other two differentiate into developing new macronuclei (anlagen), in which genome amplification and reproducible DNA rearrangements take place. The germ line chromosomes are fragmented into macronuclear chromosomes, which are healed by the addition of telomeric repeats: in some ciliates, such as *Paramecium* and, to a lesser extent, *Tetrahymena thermophila* chromosome fragmentation is associated with the imprecise elimination of germ line sequences. Furthermore, internal eliminated sequences (IESs) are excised from the chromosomes. *Paramecium* IESs are short (26 to 882 bp), noncoding, AT-rich, single-copy sequences present within coding and noncoding regions of the germ line genome (reviewed in reference 10). Their number has been estimated to be around 50,000 to 65,000 per haploid genome (8). Each IES is flanked by two 5′-TA-3′ dinucleotides, one of which remains in the chromosome after excision. A degenerate consensus sequence (5′-TAYAGYNR-3′), including the TA dinucleotide (underlined), is loosely conserved as an inverted repeat at IES ends (16). This motif is similar to the ends of Tc/mariner transposons and of "TA" IESs identified in some other ciliates (12). It has therefore been proposed that "TA" IESs have evolved from ancient transposons (17). Consistent with this hypothesis, putative transposable elements have been identified in the germ line genome of *P. aurelia* and *Euplotes crassus*, and their ends exhibit strong similarity to those of "TA" IESs (reviewed in references 13 and 22).

As a first step toward understanding the mechanism of IES excision, putative intermediate products were characterized in *P. tetraurelia* (2). Abundant double-stranded circular forms were detected for IESs longer than 200 bp. These excised circles accumulate after the massive elimination of chromosomal IESs and are then rapidly degraded (10). In these molecules, IES ends are precisely joined by one copy of the TA dinucleotide. The structures of the circular and macronuclear junctions suggest that the flanking TA dinucleotides are the target sites for the DNA cleavages initiating IES excision. A similar hypothesis was proposed for *Euplotes* "TA" IESs (18), but in neither species have DNA cleavage sites been mapped at the nucleotide level. For *Tetrahymena* IESs, however, whose structure differs from that of "TA" IESs (reviewed in reference 34), convincing evidence was obtained that excision is initiated

* Corresponding author. Mailing address: Laboratoire de Génétique Moléculaire, CNRS UMR 8541, Ecole Normale Supérieure, 46 rue d'Ulm, 75005 Paris, France. Phone: (0)1 44 32 39 47. Fax: (0)1 44 32 39 41. E-mail: betermie@wotan.ens.fr.

at either boundary by a double-strand break (DSB) producing 4-base 5′ overhangs and 3′ recessed ends terminated by an adenosine residue (27, 29). Formation of the macronuclear junction and excision of a linear molecule was proposed to result directly from the nucleophilic attack of the other boundary by the free 3′OH group carried by the broken chromosome end (28).

In the present report, we describe time course analyses of the specific developmental DNA breaks introduced at IES boundaries in starved cultures of *P. tetraurelia* undergoing autogamy, which is a self-fertilization event (31). Focusing on four IESs, we show that staggered DSBs generate free 5′PO_4 and 3′OH groups at both sides of the TA dinucleotide marking each boundary. These DSBs carry 5′ overhangs and are produced early during macronuclear development, prior to the formation of IES circles. Based on these data, we discuss a new model in which IES excision is initiated by a DSB at each boundary, which generates 4-base overhangs centered around the TA. We propose that the precise closure of macronuclear junctions relies on a repair step involving alignment and processing of the broken chromosome ends. Similarly, IES circles could result from intramolecular joining of the ends of linear excised products.

MATERIALS AND METHODS

***P. tetraurelia* strains, growth conditions, and DNA extraction.** Two independent, fully homozygous derivatives of *P. tetraurelia* strain 51 were used: 51 *new*, carrying the wild-type A^{51} gene, was obtained from a cross between wild-type strain 51 and an isogenic strain carrying the AIM2 mutation in A^{51} (21), and 51 *Gonzales* is generated by two successive backcrosses resulting in the reintroduction of the A^{51} allele into the standard laboratory strain d4.2, which is largely isogenic with 51 but carries the A^{29} allele. All experiments were repeated in both genetic backgrounds, and no difference was noted between the two strains. For time course analyses (2), each strain was grown at 27°C and autogamy was monitored by 4′,6-diamidino-2-phenylindole (DAPI) staining of cells. The $t = 0$ time point was chosen as the time when the percentage of autogamous cells reached 96% for 51 *new* and 89% for 51 *Gonzales.* At $t = 20$ h, fresh medium was added to the cultures to facilitate the progression of macronuclear development. A detailed description of the cytological states of the cultures can be found at http://www.biologie.ens.fr/perso/emeyer/paramecium.html. Total genomic DNA was extracted from 400-ml aliquots of the cultures, with a proteinase K treatment preceding the phenol extraction step (7). Aliquots of total DNA were treated with 20 μg of RNase A per ml for 30 min at 37°C and quantified by ethidium bromide staining of 1% agarose gels. Electrophoresis, Southern blotting, ^{32}P labeling of primers and PCR fragments, and hybridization procedures were as described, except that 8 μg of total genomic DNA was loaded in each lane.

Enzymes and standard procedures. Restriction enzymes, T4 polynucleotide kinase, and terminal deoxynucleotidyltransferase (TdT) were purchased from New England Biolabs and used as recommended by the supplier. The sequencing-grade *Taq* buffer (50 mM Tris [pH 9], 2 mM $MgCl_2$) was used for PCR amplification and primer extension in LMPCR assays, using the sequencing-grade *Taq* DNA polymerase (Promega) (see below). PCR amplifications were performed in 25 μl of 1× DyNAzyme buffer, with 10 pmol of each primer, 5 nmol of each deoxynucleoside triphosphate (dNTP) and 1 U of DyNAzyme II DNA polymerase (Finnzymes). The standard program was run on a Techne thermal cycler: 2 min at 95°C, 30 to 35 cycles of 1 min at 95°C, 1 min at the appropriate annealing temperature, and 1 min at 72°C, followed by a final step of 3 min at 72°C. The PCR products were analyzed on 3% NuSieve GTG agarose gels (BioWhittaker Molecular Applications).

Oligonucleotides and linkers. Gel-purified or HPSF oligonucleotides were provided by MWG Biotech or Genaxis. The sequences of all *Paramecium*-specific primers can be found at http://www.biologie.ens.fr/perso/emeyer/paramecium.html. Other oligonucleotides were I (5′-GCTCGGACCGTGGCTAGGATTAGTG-3′), J (5′-CACTAATGCTA-3′), I′ (5′-GCTCGGACCGTGGCTAGCATTAGTC-3′), J′ (5′-GACTAATGCTA-3′), and derivatives of J′ carrying various 4-base 5′ extensions. Anchor primers were 5′-GCTCGGACCGTGGCTAGCATTAGTGAGT-3′ carrying 16-base poly(dG), poly(dC), or poly(dT) 3′ extensions. Linkers (20 pmol/μl) were prepared as indicated (24), and the denaturation and cooling steps were 5 min at 95°C, 10 s at 70°C, and a slow decrease to 4°C at a rate of 1°C/min.

We performed 5′ labeling at 37°C for 30 min with a final volume of 10 μl containing 10 pmol of primer, 5 U of T4 polynucleotide kinase, and 10 pmol of [γ-^{33}P]ATP (2,500 mCi/mmol [Amersham]). Primer extension reactions were performed with a final volume of 25 μl of 1× Taq buffer with 0.5 pmol of ^{33}P-labeled primer, 5 nmol of each dNTP, and 1 U of sequencing-grade *Taq* DNA polymerase. The program used was 2 min at 95°C, 1 to 10 cycles of 1 min at 95°C, 1 min at the annealing temperature, and 1 min at 72°C, followed by a final incubation for 3 min at 72°C. Primer extension products were analyzed on 6% polyacrylamide–7 M urea sequencing gels (26).

DNA-sequencing reactions were performed manually using the *fmol* DNA cycle sequencing system (Promega) and ^{33}P-labeled primers. Alternatively, samples and primers were sent to MWG Biotech AG for automated Value Read sequencing. All sequencing templates were amplified from agarose gel slices or, for some primer extension products, from dried sequencing gels following an overnight elution at 37°C in 10 mM Tris(pH 8)–1 mM EDTA–0.5 M CH_3COONa–0.2% sodium dodecyl sulfate.

Tailing of 3′ ends. Genomic DNA (1.14 μg) was tailed with TdT in the presence of 16 μM dGTP or dCTP (or 1.6 μM dATP) by a procedure adapted from reference 27. Ethanol-precipitated tailed DNA was annealed as described with 32 pmol of the appropriate anchor primer in 40 μl of 1× DyNAzyme buffer containing 10 nmol of each dNTP. A 5-μl volume of 1× DyNAzyme buffer containing 10 pmol of primer I, 10 pmol of a specific primer, and 1 U of DyNAzyme was added to 20 μl of the annealing mix. After 1 min at 50°C and 3 min at 72°C, PCR and primer extension were carried out as indicated above, with a 3-min extension time to favor the replication of polynucleotide tails.

Detection of free 5′PO_4 ends. Ligation-mediated PCR (LMPCR) was performed as described previously (29). A 5-pmol portion of specific primer 1 was annealed to 1.14 μg of genomic DNA in 1× sequencing-grade *Taq* buffer. The 5 U of sequencing-grade *Taq* DNA polymerase and 40 nmol of each dNTP were added for complementary-strand synthesis in a final volume of 200 μl. After ethanol precipitation, nonphosphorylated linker I′/J′ (or I/J) was ligated using 3 U of T4 DNA ligase (Promega). Ethanol-precipitated ligation products were amplified by PCR with I′ (or I) and an internal primer.

Detection of DSBs. Nonphosphorylated linker I′/(nTAn)J′ (6 pmol) was ligated to 280 ng of genomic DNA, as described for the LMPCR experiment. After inactivation of T4 DNA ligase for 20 min at 65°C, free linkers were removed by purification through a QIAquick Spin Column (Qiagen Operon). One-fifth of the purified reaction mixture was used for PCR amplification of the ligated molecules, with I′ and a second specific primer.

RESULTS

Free 3′OH groups are detected at IES boundaries at early stages of macronuclear development. The presence of one TA dinucleotide at the chromosomal and circular junctions created by IES excision prompted us to look for developmental DNA cleavages at IES boundaries. Macronuclear development extends over two cell cycles separated by karyonidal division, at which time the anlagen segregate between each daughter cell (1). Previous studies with a limited number of synchronized conjugating cells demonstrated that IESs are excised within a defined time window, halfway through the first cell cycle (2). These experimental conditions, however, do not provide genomic DNA in sufficient amounts to allow the molecular study of putative intermediates produced during the excision process. We therefore used larger-scale starved cultures of *P. tetraurelia* strain 51 undergoing autogamy to prepare total genomic DNA at different time points throughout macronuclear development, focusing mainly on the first cycle. This increase in sample scale caused a slight loss in synchrony, as indicated by the detection, for each time point, of cells at different stages of macronuclear development (a supplemental figure is provided at http://www.biologie.ens.fr/perso/emeyer/paramecium.html). However, since the progression of autog-

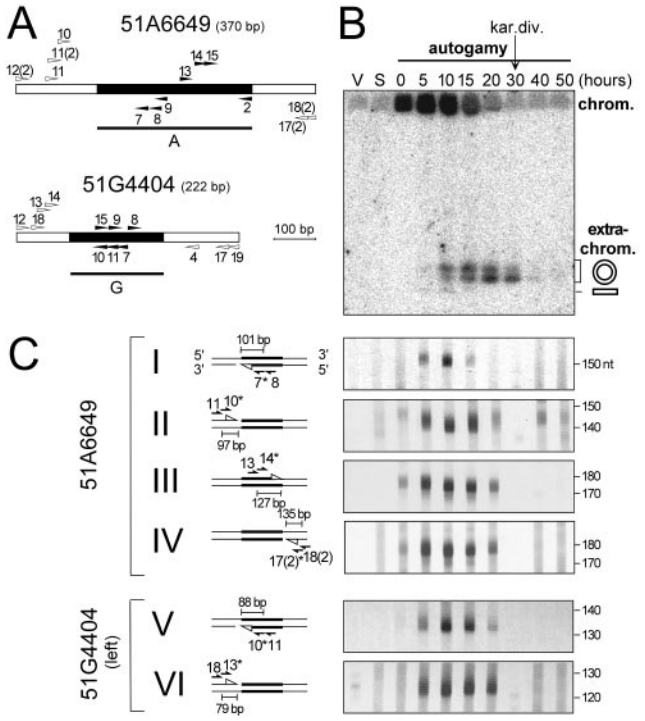

FIG. 1. Detection of free 3′OH groups at IES boundaries. (A) Maps of IESs 51A6649 and 51G4404. IESs are shown in black. Oligonucleotides are drawn as arrowheads, and hybridization probes A (bp 9215 to 9584 in GenBank sequence L26124) and G (bp 7366 to 7601 in GenBank sequence AJ010441) are indicated. (B) Timing of IES 51A6649 excision and circle degradation. A Southern blot of genomic DNA from 51 *new* was hybridized with ^{32}P-labeled probe A and revealed on a fluorimager imaging plate. V, vegetative cells (1,000 cells/ml); S, starved vegetative cells (3,200 cells/ml); kar. div. karyonidal division; chrom., chromosomal bulk; (C) Poly(dG) tailing of free 3′ ends for IESs 51A6649 and 51G4404. ^{33}P-labeled primer extension products were separated on sequencing gels, and autoradiograms are shown. Both DNA strands are drawn, with bold lines corresponding to IESs and arrowheads symbolizing free 3′OH groups. Primers are shown as arrows, with an asterisk marking those used for primer extension. For 51G4404, only the results obtained for the left boundary are shown. The distances between the 5′ end of each primer and the TA dinucleotide at the IES boundary are shown in each diagram. The sizes of the primer extension products, estimated according to a sequencing ladder obtained from the same primers and run on the same gel, reflect the additional contribution of the poly(dG) extension and of the anchor primer used in the assay.

amy could be observed in the population of cells, the resulting DNA preparations were used for all experiments described in this study. Southern blot hybridization with IES probes (Fig. 1A and B and data not shown) confirmed our previous observations (2, 10) that IESs are first amplified within the bulk of chromosomal DNA, excised, and accumulated as extrachromosomal molecules that are finally eliminated after karyonidal division.

In a first approach, since no assumption could be made a priori regarding the exact position or the nature of the breaks (single or double stranded), we searched for free 3′OH groups on each strand around the TA dinucleotides conserved at IES boundaries. Genomic DNA was heat denatured to expose 3′ ends, and poly(dG) extensions were added with TdT. Poly(dG)-tailed molecules were amplified by PCR, using an anchor primer carrying a poly(dC) 3′ tail and a second strand-specific primer at each IES boundary. Nested primer extensions allowed high-resolution analysis of the PCR products. The results obtained for IES 51A6649 and the left end of 51G4404, located in surface antigen genes A^{51} and G^{51}, respectively (23, 25), are displayed in Fig. 1C. While no specific primer extension product is detected in the vegetative controls (V and S), the liberation of 3′OH groups is apparent during autogamy, at each IES end and on both DNA strands. All free 3′ ends exhibit a similar timing of appearance for 51A6649 and 51G4404 (Fig. 1C and data not shown): they are detected early in autogamous cells ($t = 0$), reach a peak when two anlagen are revealed by DAPI staining ($t = 10$ h), and then disappear. Interestingly, the maximal level of free 3′OH ends is reached approximately 10 h before the maximal accumulation of excised IES circles ($t = 20$ h). In addition, close examination of the primer extension products reveals that a smear of bands can be distinguished for each time point. This may reflect either variations in the length of the polynucleotide tail added to a defined 3′ end or alternative positions for the free 3′OH groups used as substrates for tailing.

Sequences of the 3′-tailed products. To map precisely the 3′ ends to which the polynucleotide extension had been added, the tailing was repeated with poly(dG), poly(dA), or poly(dC) to avoid sequencing ambiguities due to the sequence context, and the specific PCR products were sequenced. The results obtained for IES 51G4404 are shown in Fig. 2. Starting from inside the IES, unique positions were detected for the tailing of the left and right ends, 1 nucleotide (nt) 5′ to the flanking 5′-TA-3′ (Fig. 2A and B). On the macronuclear side of each TA, however, a double peak is conspicuous on the sequence chromatograms, at the site where the polynucleotide tail is branched (Fig. 2A). Since no double peak was found when the same extension was added to a control fragment of gene G^{51}, precleaved with *Asp*718 at the macronuclear junction formed after IES 51G4404 excision (Fig. 2C), we conclude that two 3′ ends are formed on the macronuclear side of the TA (Fig. 2B). One of these is located 1 nt 5′ to the TA, in a symmetrical position relative to the unique 3′ end liberated inside the IES. The additional end is immediately upstream from the TA. The same analysis was performed for IES 51A6649, and, again, a single free 3′ end was detected on the IES side of each TA whereas two were found on the macronuclear side (Fig. 2B).

5′PO$_4$ groups are liberated at two alternative positions at IES ends. The two free 3′OH groups detected on the macronuclear side of the TA may be generated either by the cleavage of one of two alternative phosphodiester bonds or by 3′-end processing of one molecule cleaved primarily at a unique site. To investigate this point, we first asked whether corresponding 5′ ends could be detected on the macronuclear side of the TA in an LMPCR. Genomic DNA from autogamous cells was heat denatured, and one round of DNA synthesis was performed from a primer specific for either end of IES 51G4404 (Fig. 3A). A blunt-ended linker was ligated to the resulting blunt-ended molecules, and specific ligation products were amplified by PCR and used as substrates for primer extensions. High-resolution analysis on sequencing gels (Fig. 3B) reproducibly revealed a doublet of bands (U and L in panels I and II) for each IES end at early stages of macronuclear development ($t = 5$ h to $t = 20$ h). The maximum level was reached at t = 15 to 20 h

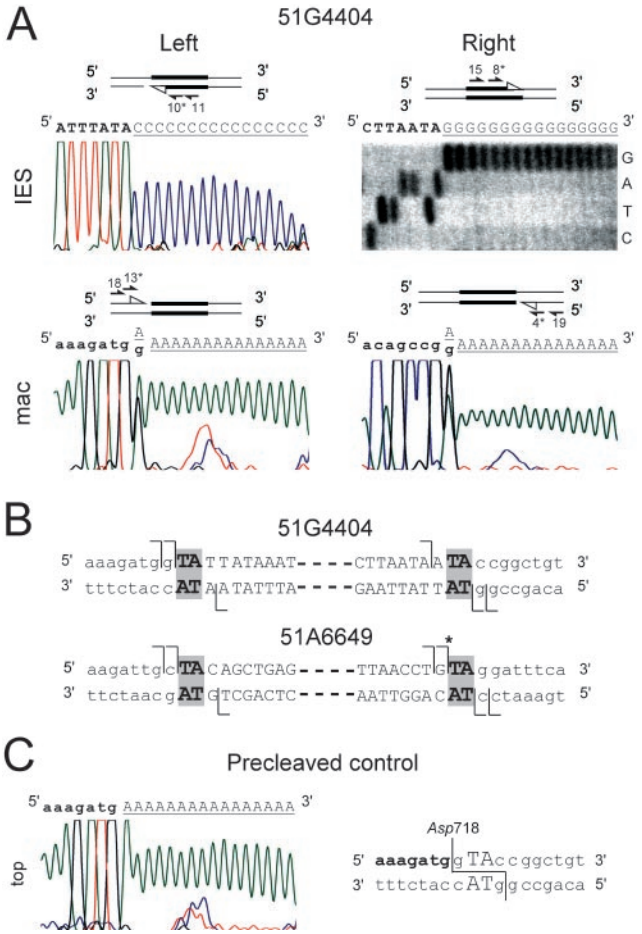

FIG. 2. Mapping of the free 3′ ends at the boundaries of IESs 51G4404 and 51A6649. (A) Sequencing of the tailed products for 51G4404. DNA-sequencing chromatograms are shown except for the top right panel, in which an autoradiogram of a sequencing gel is presented. For the IES sides, poly(dC) was added to the left end and poly(dG) was added to the right. Macronuclear sides were tailed with poly(dA). All sequences were obtained with the $t = 10$ h sample (Fig. 1), but no significant difference was observed for other time points. PCR and sequencing primers (*) are indicated on the diagrams. The IES sequence is written in capital letters, and the flanking macronuclear sequence is written in lowercase letters. Polynucleotide extensions are underlined. (B) Localization of free 3′ ends around the TAs flanking IESs 51G4404 and 51A6649. The terminal nucleotides of IES ends are displayed in capital letters, with the flanking TA in bold, and the internal part of each IES is represented by a dotted line. Macronucleus-destined sequences are written in lowercase letters. For 51A6649, PCR primers were A8 (IES left), A13 and nested primer A14 (IES right), A12(2) (mac left) and A18(2) (mac right). Sequencing primers were A7 (IES left), A15 (IES right), A11(2) (mac left) and A17(2) (mac right). A sequence ambiguity (indicated by an asterisk) at the right end of IES 51A6649 could not be resolved. (C) DNA sequencing chromatogram of the *Asp*718-precleaved DNA fragment, carrying the macronuclear sequence of gene *G*[51], tailed with poly(dA). The fragment was mixed with DNA from starved vegetative cells prior to TdT treatment. See panel A for the primers specific for the macronuclear left side of the TA.

in the experiment in Fig. 3B, approximately 10 h before the maximal accumulation of excised IES circles ($t = 25$ h in panel IV). Additional primer extension products were detected (panels I and II), but these were not reproducible and could not be attributed to any specific molecule. Sequencing of the gel-

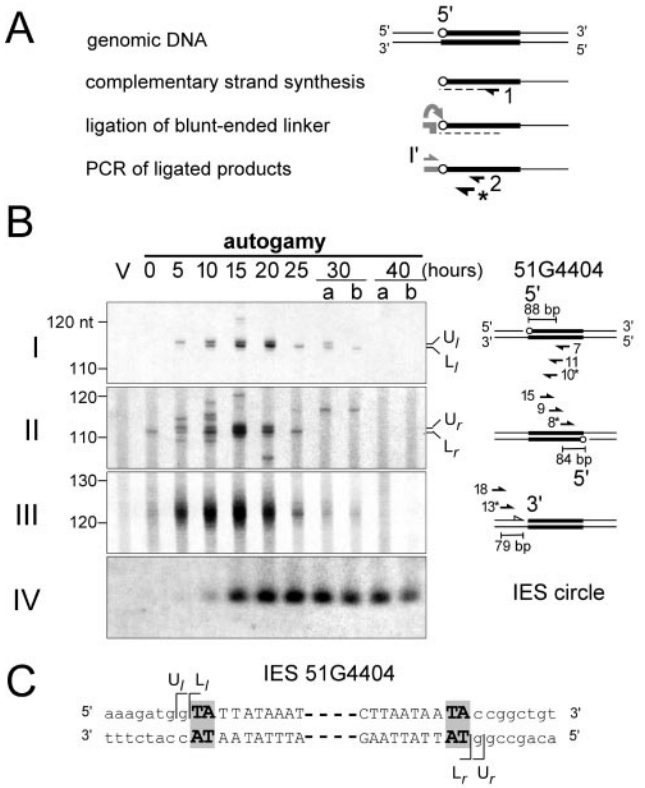

FIG. 3. LMPCR detection of 5′PO_4 groups at the ends of IES 51G4404. (A) Strategy for the detection of free 5′ phosphorylated IES ends. IES-specific primer 1 is annealed to denatured genomic DNA and extended for complementary strand synthesis with sequencing-grade *Taq* DNA polymerase (dotted line). This enzyme often adds a nontemplated extra A residue to the 3′ end of the newly synthesized strand, which may restrict the efficiency of blunt-end formation (9), but has a very low 5′-to-3′ exonuclease activity. Thus, any ligation event reflects the existence of a free 5′ PO_4 group in the input genomic DNA. Linker I′/J′ (in gray) is ligated to the resulting double-stranded end, and the ligated molecules are amplified with I′ and primer 2 (internal to the IES). A ^{33}P-labeled IES-specific primer (marked with an asterisk) is used for primer extension or sequencing of the amplified ligation product. Both DNA strands are drawn, with bold lines corresponding to the IES and the free 5′PO_4 group symbolized by a circle. (B) Panels I and II show autoradiograms of sequencing gels showing the primer extension analysis of LMPCR products for IES 51G4404. Total genomic DNA was extracted from a vegetative culture of 51 *Gonzales* (V: 1,000 cells/ml) or from autogamous cells. After addition of fresh medium to an aliquot of the culture, the starved (lanes a) and refed (lanes b) cells were analyzed in parallel at $t = 30$ h and $t = 40$ h. The sizes of the primer extension products, estimated according to a sequencing ladder run in parallel, correspond to the sum of the length of oligonucleotide I′ from the linker (25 bp) and of the distance separating the primer 5′ end and the linker ligation site at the IES boundary (shown in each diagram). For each end, the upper band (U_l and U_r) of the doublet represents the detection of a 5′PO_4 group one nucleotide 5′ to the TA on the macronuclear side (see also panel C), whereas the lower band (L_l and L_r) corresponds to the 5′ terminal TA. As a control, the free 3′OH groups on the macronuclear side of the left TA were revealed by poly(dG) tailing and primer extension analysis: an autoradiogram of the resulting sequencing gel is shown in panel III (see Fig. 1 for details of size determination). Excised IES circles (222 bp) were detected by Southern blot hybridization of an agarose gel with ^{32}P-labeled probe G (panel IV) (Fig. 1). (C) Mapping of the free 5′PO_4 groups at IES 51G4404 ends. See the legend to Fig. 2B.

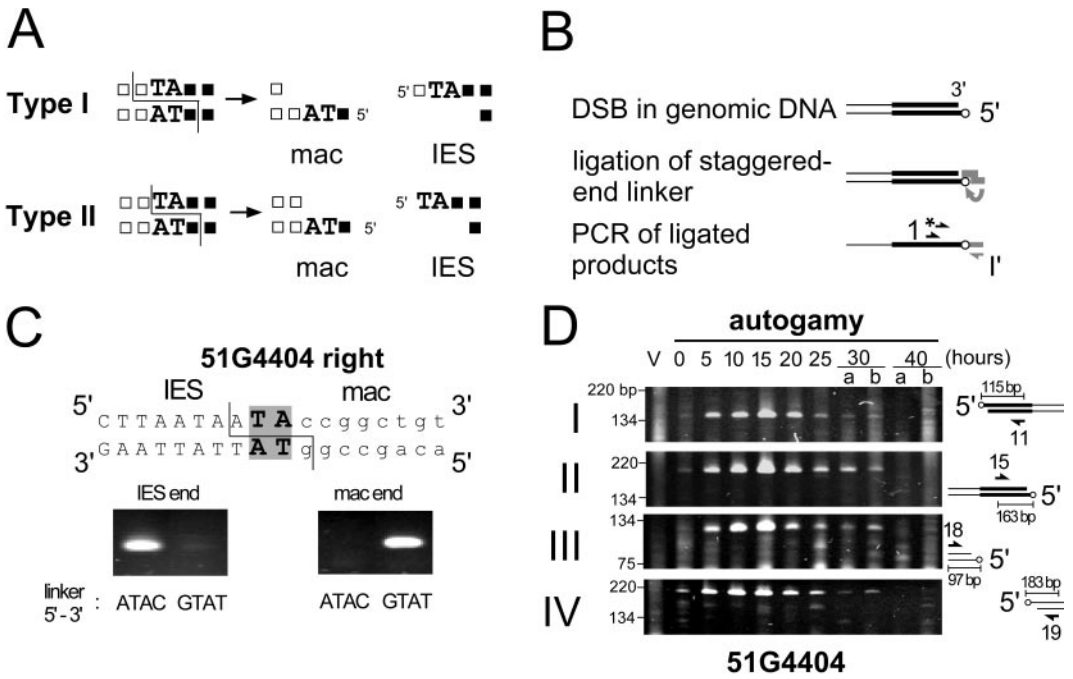

FIG. 4. DSBs at IES boundaries during macronuclear development. (A) Structure of the putative DSBs deduced from the mapping of individual 3′ and 5′ ends. The macronuclear side of the TA is represented by white squares, while IES-specific nucleotides are drawn as black squares. (B) Strategy used for DSB detection. Linker I′/(nTAn)J′ (in gray) is ligated to genomic DNA. Pairing of the nonphosphorylated 5′-nTAn-3′ extension aligns the 3′ end of I′ with the 5′ protruding end of the genomic DNA and allows their ligation. The ligated strand is amplified with I′ and specific primer 1. A ^{33}P-labeled primer (marked with an asterisk) is used for primer extension of PCR products. The 5′PO_4 residue involved in ligation is drawn as a circle, and bold lines represent IES sequences. The same strategy applies to macronucleus-destined ends. (C) Assay for the specificity of ligation of linkers I′/(ATAC)J′ (designed for the detection of IES ends) and I′/(GTAT)J′ (designed for the macronucleus-destined ends) to the IES and macronucleus-destined ends at the right boundary of 51G4404. The sequence of the boundary and the position of the predicted type I cleavage are displayed at the top of the panel. Ethidium bromide-stained agarose gels of the PCR products amplified from linker ligation reactions using the 51 *Gonzales* $t = 10$ h sample are shown (Fig. 3B), with the IES end amplified from primer G15 and the macronucleus-destined end from G19 (see panel D). The 4-base extension of the linker used in each reaction is indicated below the corresponding lane. (D) Time course analysis of DSBs at the boundaries of IES 51G4404. Macronuclear development was monitored during autogamy of 51 *Gonzales* (Fig. 3B). Linker ligation products were amplified by PCR using the specific primers diagrammed on the right of each panel and detected on ethidium bromide-stained agarose gels. Relevant size markers from a 1-kb DNA ladder (Gibco-BRL) are indicated on the left of each panel. The size of each PCR product corresponds to the distance separating the 5′ end of the primer from the corresponding IES boundary (displayed on each diagram) plus the size of primer I′ (25 bp) from the linker.

purified doublets confirmed that ligation of the linker occurred at two alternative positions on each strand, 1 nt upstream of (U) or immediately 5′ to (L) the TA (Fig. 3C). Since the linker was not phosphorylated, any ligation event observed in these experiments is strictly dependent on the presence of free 5′PO_4 groups on the genomic DNA. These 5′PO_4 groups were detected at the same time points as the 3′ ends liberated on the same strand (Fig. 3B, panel III, and data not shown). In addition, a comparison with Fig. 2B reveals that the positions of the 5′ and 3′ ends coincide, which suggests that one of two consecutive phosphodiester bonds can be hydrolyzed alternatively on the macronuclear side of the TA.

Developmental DSBs at IES boundaries. We asked whether the developmental breaks detected on each strand could be introduced on the same DNA molecule, thus generating DSBs. According to the mapping of free ends on the macronuclear side of each TA, two structures may be proposed for the staggered ends generated by putative DSBs (Fig. 4A). In type I DSBs, symmetrical 4-base 5′ overhangs centered on the TA are created at the ends of macronucleus-destined and IES sequences. In contrast, when compared to each other, the two 3-base 5′ overhangs generated by type II DSBs at the macronucleus and IES-destined ends are asymmetric relative to the TA: at IES ends, the free 5′PO_4 group is located on the T residue of the conserved dinucleotide, while at macronucleus-destined ends an additional residue is present 5′ to the TA. In a first approach, we searched directly for type I DSBs by using a strategy based on the ligation of linkers carrying 5′ protruding ends complementary to the predicted free ends, followed by PCR amplification of the resulting ligation products (Fig. 4B). Linkers with 4-base 5′ overhangs were designed to hybridize to the type I DSBs predicted for IES 51G4404: linker I′/(ATAC)J′ is complementary to both IES ends, and linker I′/(GTAT)J′ is complementary to the macronucleus-destined ends. In the assay, because the 5′ overhangs of the linkers are not phosphorylated and cannot be ligated, the detection of PCR products reflects ligation, on one strand only, of the 3′ end of oligonucleotide I′ to the phosphorylated free 5′ end of the DSB. In addition, a control experiment confirmed that ligation is strictly dependent on correct pairing between the 4-base extension of the linker and the 5′ overhang of the DSB, since no signal was obtained for IES ends when the macronu-

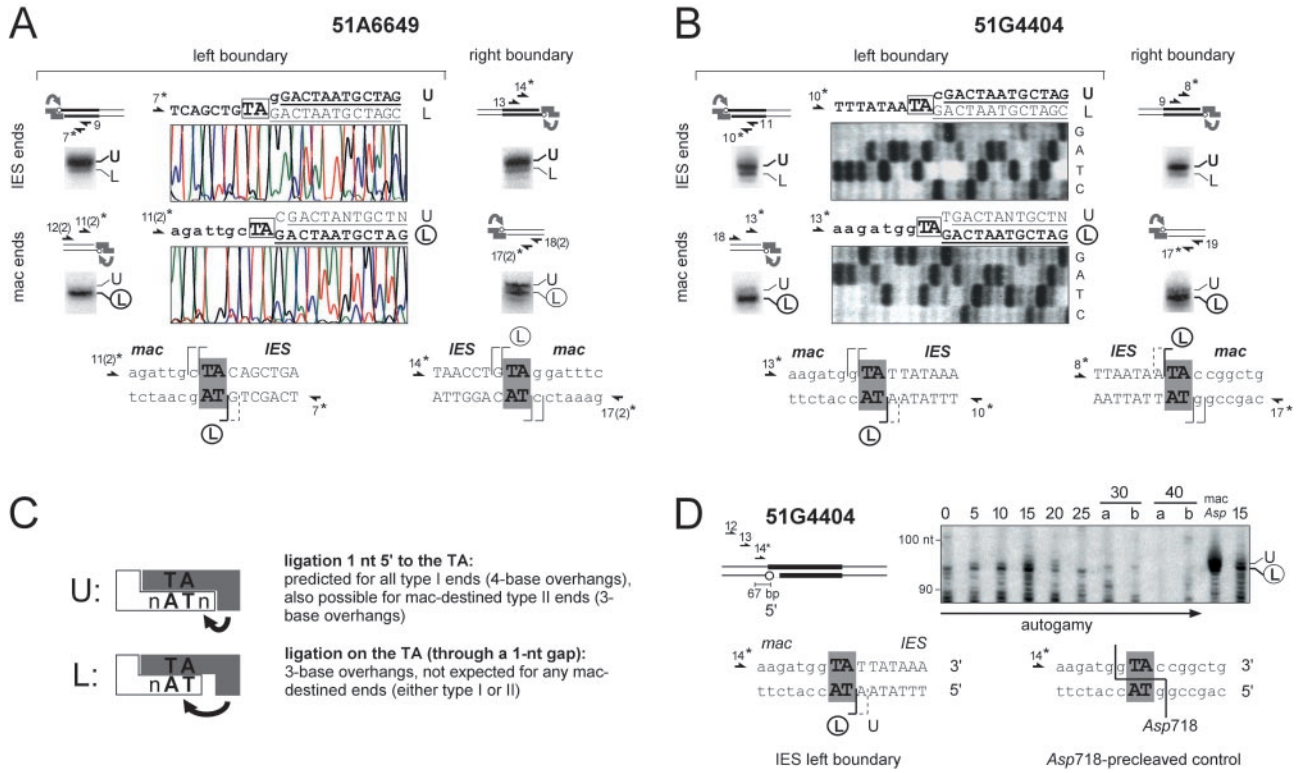

FIG. 5. DSBs at IES boundaries generate 3- and 4-base overhangs. (A and B) Primer extension and sequencing analysis of the linker ligation products obtained for IESs 51A6649 (A) and 51G4404 (B). Genomic DNA from autogamous 51 *new* at $t = 10$ h (Fig. 1B) was ligated to linkers I′/(GTAG)J′ (IES ends) or I′/(CTAC)J′ (mac ends) for 51A6649 and to I′/(ATAC)J′ (IES ends) or I′/(GTAT)J′ (mac ends) for 51G4404. The positions of all primers are shown on the diagrams, with an asterisk marking those used for primer extension and sequencing. IES sequences (capital letters) are represented by thick lines, and flanking macronuclear sequences (lowercase letters) are represented by thin lines. All ^{33}P-labeled primer extension products were analyzed on sequencing gels and revealed by autoradiography. Sequencing chromatograms (for 51A6649) or sequencing gels (for 51G4404) are shown for the left boundary of each IES. The sequence of the strand complementary to the one on which ligation has taken place is displayed above each panel, with the major sequence in bold and the linker underlined. Product U corresponds to linker ligation on the nucleotide 5′ to the TA, while L corresponds to ligation on the T residue (each circled L represents the unexpected major ligation product observed for the macronucleus-destined ends). (C) Ligation reactions leading to products U and L, with the linker in gray and *Paramecium* genomic DNA ends in white. (D) LMPCR detection of free 5′PO_4 groups on the IES side of the TA, at the left boundary of IES 51G4404. The *Asp*718-precleaved control fragment was mixed with DNA from vegetative cells, and genomic DNA samples were as in Fig. 3. The experimental strategy was as for Fig. 3A, except that linker I/J and primers hybridizing within macronuclear flanking sequences were used. An autoradiogram of the sequencing gel used for the detection of primer extension products is shown, with the positions of size markers (from a sequencing ladder) indicated on the left. In this experiment, bands U and L were labeled following the same rule as in Fig. 3B and correspond to the same positions as linker ligation products U and L, respectively, detected at macronucleus-destined ends in panel B. Their observed sizes are consistent with the estimation of the distance separating the 5′ end of the primer from the IES boundary (indicated on the diagram), incremented by the 25 bp from linker primer I.

cleus-specific linker was used, and vice versa (Fig. 4C). A time course analysis revealed that, specifically during macronuclear development, DSBs are produced both at macronucleus-destined and IES-specific ends, for IES 51G4404 (Fig. 4D), with the same timing as individual 3′OH and 5′PO_4 free ends on each strand (Fig. 3B). Identical results were obtained for IES 51A6649 (data not shown). To search for type II DSBs, we reasoned that they could be distinguished from type I DSBs by the 5′ residue present at the IES ends (Fig. 4A). Therefore, we used linker I′/(ATA)J′, specific for the type II IES ends predicted for 51G4404, and, indeed, detected specific PCR products (not shown). Thus, type I and II DSBs are found at the boundaries of *Paramecium* IESs and accumulate approximately 10 h before the circular excised molecules do.

Unexpected 3-base 5′ overhangs are formed at macronucleus-destined ends. To check the correct ligation of the linkers, the PCR products obtained for IESs 51G4404 and 51A6649 were analyzed by primer-extension and sequencing. The detection of primer extension products on high-resolution sequencing gels followed the same timing as observed for ethidium bromide-stained PCR products (data not shown). For each type I DSB, two labeled bands (U and L) were identified (Fig. 5A and B), and their relative amounts remained essentially constant throughout macronuclear development (data not shown). Direct sequencing of the PCR products revealed two mixed sequences, shifted by 1 base relative to each other, that correspond to the two primer extension products U and L (Fig. 5A and B). For IES ends (top panels), major band U reflects ligation of the linker to the terminal base of the predicted 4-base 5′ overhang while band L results from ligation immediately 5′ to the TA, which, for a 4-base linker, has to occur through a 1-nt gap (Fig. 5C). For IES 51G4404, these

two positions are in agreement with the data obtained from the LMPCR analysis of individual 5′ free ends on the macronuclear side of the TA (Fig. 3C) and the structure of product L is consistent with the direct detection of type II DSBs at IES ends with linker I′/(ATA)J′ (data not shown). Strikingly, for macronucleus-destined ends, although the expected 4-base extensions can also be detected (band U), the major primer extension product is band L (Fig. 5A and B, bottom panels), with, perhaps, the exception of the macronucleus-destined right end for IES 51A6649. Sequencing analysis confirms that band L corresponds to ligation of the 4-base linker 5′ to the TA and, again, involves the formation of a gapped ligation intermediate. Taking into account that ligation through a 1-nt gap is probably less efficient than ligation to a fully complementary 4-base overhang, we conclude that most of the DSBs detected with the type I linker at macronucleus-destined ends exhibit a 5′ terminal TA dinucleotide. Moreover, no ligation product was obtained with linkers I′/(ATAC)J′ (Fig. 4C) and I′/(ATAT)J′ (data not shown) on the macronucleus-destined ends released at the boundaries of IES 51G4404. Therefore, the 5′-terminal nucleotide of the linker has to pair with a facing complementary nucleotide, located on the macronuclear side of the TA on the single-stranded extension of the DSB, to allow ligation of oligonucleotide I′ through a 1-nt gap [which is the major event observed with linker I′/(GTAT)J′ in Fig. 4C]. Thus, most macronucleus-destined ends detected by the ligation of 4-base linkers exhibit a 3-base recessed 3′OH end and a 5′-TAN overhang. This was totally unexpected since, in both type I and II DSBs, macronucleus-destined ends should carry an additional base 5′ to the TA (Fig. 4A).

To confirm the data obtained in the linker ligation assay for the macronucleus-destined broken ends, we used LMPCR (Fig. 3) to search for individual 5′PO_4 ends on the IES side of the TA, at the left boundary of IES 51G4404. Because primers hybridizing to the flanking macronucleus-destined sequences were used in this experiment, we observed quite a high background of macronucleus-specific bands, probably due to the presence of large amounts of macronuclear DNA in our preparations (the macronucleus is ~800N in *P. tetraurelia*), as was also noted by other authors who used the same technique with *Tetrahymena* (29). Two developmental LMPCR products were detected, whose lengths differed by 1 nt (Fig. 5D). As judged by its relative mobility compared to an *Asp*718-precleaved control, which exhibits an additional base 5′ to the TA, we conclude that the major, faster-migrating LMPCR product (band L) lacks this additional nucleotide and corresponds to ligation on the 5′ T residue.

Taken together, the results obtained with IES 51G4404 and 51A6649 indicate that on the IES side of the TA, only the minor 5′PO_4 group coincides with the unique 3′OH free group detected by TdT extension whereas the major 5′PO_4 group liberated on the T residue (circled L in Fig. 5) does not colocalize with any detectable 3′OH end (Fig. 6A). In an attempt to generalize this intriguing observation, we examined two other IESs, 51A-712 (25) and 51A-4814 (GenBank accession no. AY228755 [J. Forney and E. Snodderley, personal communication]), located upstream from the A^{51} gene. Linkers carrying 4-base 5′ extensions [I′/(GTAT)J′ for 51A-712 and I′/(TTAC)J′ for 51A-4814] were used to analyze the macronucleus-destined protruding ends generated at the left boundary of each IES. The pattern observed for IES 51A-712 was similar to those described for 51G4404 and 51A6649: the major product corresponded to linker ligation to a 3-base extension, 5′ to the TA on the IES side (Fig. 6B). In contrast, the predicted 4-base extension was clearly detected for IES 51A-4814 and represented the most abundant ligation product.

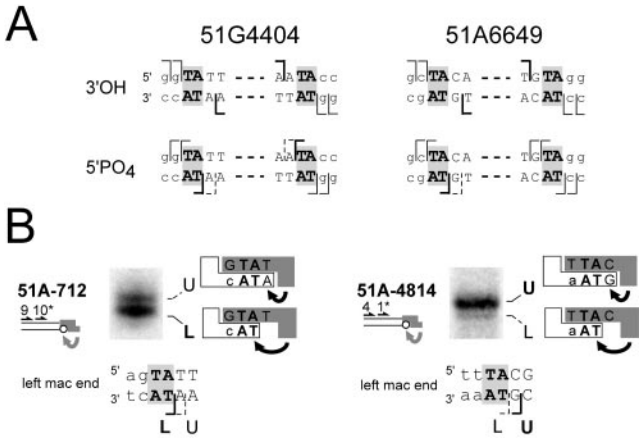

FIG. 6. Analysis of the free ends detected at the boundaries of IESs 51G4404, 51A6649, 51A-712, and 51A-4814. (A) Localization of free 3′OH and 5′PO_4 groups at the boundaries of IESs 51G4404 and 51A6649. Nucleotides on the macronuclear side of each TA are in lowercase letters, and those on the IES side are in capital letters. Minor positions for free ends are indicated by thin dotted lines, and major positions are indicated by bold lines. For clarity, the putative additional 3′ end corresponding to a sequence ambiguity at the 51A6649 right boundary has been omitted (Fig. 2B). (B) Linker ligation to the macronucleus-destined ends formed at the left boundaries of IESs 51A-712 and 51A-4814. Autoradiograms of sequencing gels detecting primer extension products obtained from 51 *new* at $t = 10$ h (Fig. 1B) are shown for each IES, with the primers drawn as in Fig. 5. The structure of the linker ligation intermediates is shown on the right of each panel, with the linkers in gray and the macronucleus-destined ends in white. Bands U and L are labeled as in Fig. 5B, with the major product designated by a bold letter.

To take these data into account, two positions may be proposed for the initial cleavage introduced on the IES side of the TA. Cleavage 5′ to the TA could generate the major 5′PO_4 group observed at macronuclear ends for IESs 51A6649, 51G4404 (Fig. 5A and B), and 51A-712 (Fig. 6B). However, this hypothesis alone cannot explain the presence of an additional 5′-terminal base (originating from inside the IES) on the macronucleus-destined 5′ overhang, which is detected for all IESs tested, most conspicuously for IES 51A-4814 (Fig. 6B). Indeed, this would require the addition of 1 nt to the cleaved 5′ end, in an unlikely 3′→5′ polymerization step. Therefore, the existence of 5′ extensions carrying an extra nucleotide 5′ to the TA implies that at least on a fraction of the molecules, initial phosphodiester bond cleavage takes place at an alternative position located 1 nt 5′ to the TA on the IES side.

DISCUSSION

Excision of *Paramecium* IESs involves staggered double-strand cleavage at both ends and DSB repair. The present study demonstrates that early during macronuclear development, double-strand cleavages producing 5′ overhangs are in-

troduced within 4 bp centered on the TA dinucleotide at each IES boundary.

On the IES side of the TA, only the 5′PO_4 group located 1 nt 5′ to the TA coincides with the unique 3′OH free group detected by TdT extension (Fig. 6A). As pointed out in Results, this position can readily be attributed to an initial cleavage releasing a 3′ end within the IES. The origin of the free 5′PO_4 group on the T residue is more difficult to interpret. It could reflect an intrinsic ability of the excision machinery to cleave one of two alternative phosphodiester bonds, as was recently reported for the transposase-induced 3′ end cleavage of the *mariner* element, Mos1 (6). The corresponding 3′ end would not be detected in our assay, perhaps because it does not carry a OH group and/or because it is processed rapidly to yield the unique 3′OH group observed at the other position. However, although this possibility cannot be ruled out definitively, it does not provide a straightforward explanation for the smaller number of macronucleus-destined 5′ overhangs terminated with a 5′-TA that are formed in the particular case of IES 51A-4814 (Fig. 6B). Indeed, assuming that the excision machinery cuts all IES ends in the same manner, we should have observed similar cleavage patterns for all IESs, including IES 51A-4814. Therefore, we rather favor a model in which an initial cleavage is introduced mainly 1 nt 5′ to the TA on the IES side and is followed by removal of the 5′-terminal nucleotide originating from inside the IES, to yield the 5′-phosphorylated TA carried by the macronucleus-destined 5′ end. As discussed below, we propose that this 5′-processing step is linked to the precise closure of the macronuclear junction and does not take place with the same efficiency for all IESs (e.g., 51A-4814). Analysis of IESs 51G4404 and 51A6649 reveals that on the macronuclear side of each TA, free 5′PO_4 and 3′OH groups are released at two positions, 5′ of the TA and 1 nt upstream, again suggesting that one of two alternative phosphodiester bonds can be cleaved (Fig. 6A). Therefore, at this stage of the discussion, two types of initiating DSBs may be generated at IES boundaries: type I DSBs carry 4-base overhangs with a central TA, while type II DSBs exhibit asymmetric 3-base overhangs with a 5′-terminal TA at IES ends and an extra residue 5′ to the TA at macronucleus-destined ends (Fig. 4A).

Models for IES excision can be grouped in two categories, according to whether one or both boundaries are cleaved as the initiating step (discussed in references 10 and 13). In the first set of models, such as those proposed for *Tetrahymena* and *Oxytricha*, excision starts with a DSB at one boundary, followed by direct strand transfer to the second one, to form one strand of the macronuclear chromosome junction (Fig. 7A). To account for the precise formation of *Paramecium* macronuclear junctions, this type of model would impose strict constraints on the positions of the two free 3′OH groups involved in the strand transfer reaction. The nucleophile group should be on the macronuclear 5′ side to the TA at the first cleaved boundary: this could be achieved either by an initial type II cleavage or by a partial fill-in of a macronucleus-destined 3′ recessed type I end. Strand transfer should expose another 3′OH group immediately 5′ of the TA at the second IES end, which is not detected in our experiments (Fig. 6A). Therefore, our data support an alternative mechanism, different from those previously proposed for *Tetrahymena* or *Oxytricha*, in which two

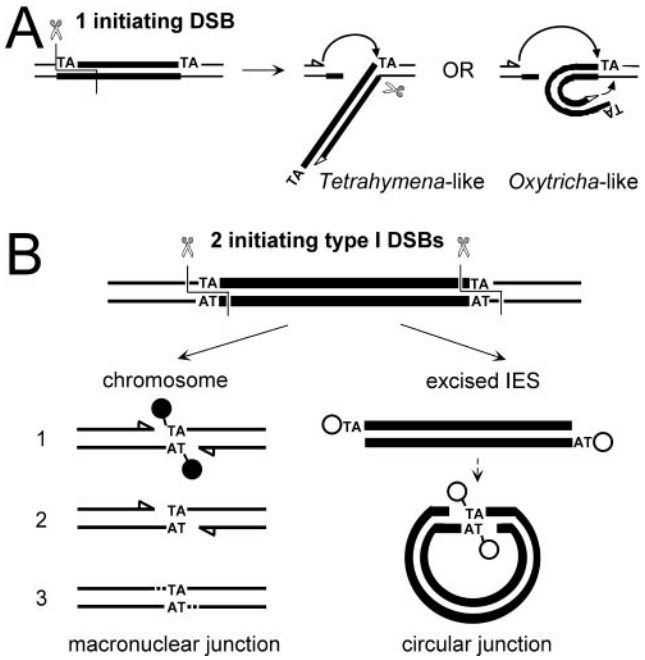

FIG. 7. Model for IES excision in *Paramecium*. (A) Excision models involving one initiating DSB at a single IES end, based on those proposed for *Tetrahymena* (28) and *Oxytricha* (33). In both models, the upper strand of the macronuclear junction is formed following the nucleophilic attack of the second boundary by the 3′OH group (white arrowheads) liberated by the initiating DSB on the macronucleus-destined end: this transesterification reaction is symbolized by an arrow. In the *Tetrahymena* model, second-strand cleavage releases a linear excised molecule, whereas in the *Oxytricha* model, another transesterification involving the first broken IES end generates a nicked circle. Both IES strands are drawn as thick lines; thin lines represent the flanking macronucleus-destined DNA. (B) Model for IES excision involving a type I DSB at both ends and subsequent DSB repair. The 5′ nucleotide of each 4-base overhang is indicated by a circle. After double-strand cleavage, broken chromosome ends (thin lines) align within a junction repair intermediate (step 1), and the macronuclear junction results from the processing of the 5′ flapped nucleotides (step 2), fill-in of the 3′ recessed ends (dotted lines in step 3), and ligation. The ends of the linear excised IES (thick lines) may be joined within a similar intramolecular intermediate to give the circles.

DSBs, one at each boundary, initiate the excision of *Paramecium* IESs (Fig. 7B). We propose that precise formation of the macronuclear junction is achieved in a second step, within a DSB repair intermediate, in which the left and right macronucleus-destined protruding ends align through the pairing of their conserved TA dinucleotides.

Chromosome healing through alignment and processing of 4-base overhangs. In the DSB repair intermediate proposed in Fig. 7B for the closure of the chromosomal junction, the 5′-terminal residue of each single-stranded extension of macronucleus-destined ends (generated by either type I or II cleavages), which originates from within the IES, would generally not pair with its facing nucleotide (51G4404 in Fig. 8A). Joining of the aligned chromosome ends would then require the processing of each 5′ flapped nucleotide, prior to gap filling from the recessed 3′ ends (for type I DSBs only) and ligation (Fig. 7B). For IESs 51G4404 and 51A6649, the two 5′PO_4 free groups detected on the IES side of the TA and the two 3′OH

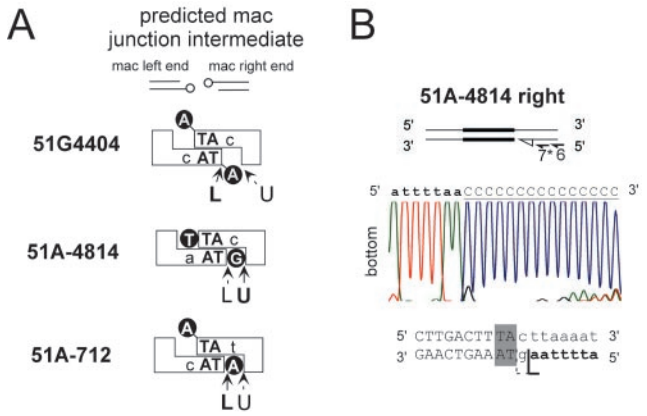

FIG. 8. Processing of macronucleus-destined ends: a correlation with their mispairing within the predicted junction intermediate. (A) Structure of the predicted junction intermediates resulting from the alignment of the two macronucleus-destined ends produced by initiating double-strand cleavages at the boundaries of IESs 51G4404, 51A-4814, and 51A-712. The broken chromosome arms are drawn at the top of the figure. In each junction intermediate, only the sequence of their aligned 4-base 5′ overhangs is shown, with the 5′ terminal residue represented by a black circle. The position and the relative abundance of the free $5'PO_4$ groups corresponding to products U and L detected in the experiments shown in Fig. 5B and 6B are given. (B) 3′ tailing of the right macronucleus-destined end for 51A-4814. Poly(dC) was added to genomic DNA of 51 *new* at $t = 10$ h. The PCR product amplified with primers -4814A6 and I was sequenced with primer -4814A7 (marked with an asterisk). The resulting sequencing chromatogram is shown (see the legend to Fig. 2).

free groups detected on the macronuclear side (Fig. 6A) would reflect 5′- and 3′-processing intermediates of the macronucleus-destined broken ends and would fit nicely with this model.

The question remains whether type II DSBs result from the processing of type I DSBs by the addition of 1 nt to the 3′ recessed macronucleus-destined ends (and the removal of the 5′-terminal nucleotide from the IES protruding ends) or whether both types are produced directly, as alternative initiating steps of IES excision. This second hypothesis would be reminiscent of the alternative 5′-end cleavage previously reported for some transposons (e.g., for the mariner-related transposon Himar1 [19, 20]). It is, however, not supported by the data obtained for IES 51A-4814, for which cleavage site mapping on the macronuclear side of the TA was based on the analysis of free 3′ ends, since the small size of this IES (28 bp) does not allow the design of internal primers necessary for LMPCR analysis of the corresponding free 5′ ends. As demonstrated by TdT tailing, the 3′ ends predicted for type I DSBs are indeed largely predominant for this IES (Fig. 8B). Therefore, assuming that the same initiating cleavages are introduced at all IES boundaries by the excision machinery, we propose that type I DSBs are the major initial products of the reaction. For IES 51A-4814, type I DSBs would generate perfectly complementary 4-base overhangs (Fig. 8A) and no fill-in of the macronucleus-destined recessed 3′ ends should be needed prior to chromosomal junction closure. Our experimental data are in full agreement with this prediction. Furthermore, the most conspicuous ligation product obtained with the type I linker I′/(TTAC)J′ on the left macronucleus-destined end of IES 51A-4814 corresponds to the expected 4-base overhang (Fig. 6B). As stated above, this indicates that trimming of the 5′-terminal residue is reduced and confirms that this nucleotide is able to pair with its facing residue within the junction intermediate. Interestingly, processing of both strands is observed even if a 5′ flap is formed on only one strand, as demonstrated for IES 51A-712 (Fig. 6B and 8A), which suggests that the reaction is symmetrical on both strands.

Fate of excised IESs. The present study indicates that the cleavages at IES boundaries are detected early: between $t = 0$ h and $t = 20$ h, with a maximum at $t = 10$ h, for the experiment in Fig. 1 (strain 51 *new*), and between $t = 0$ h and $t = 30$ h, with a maximum at $t = 15$ to 20 h, for the experiment in Fig. 3 (strain 51 *Gonzales*). These relatively large time windows most probably reflect the imperfect synchrony of macronuclear development observed in a population of autogamous cells. Previous time course analyses of IES excision have revealed that excised IESs longer than 200 bp accumulate as circular molecules (2, 10). Here, the accumulation of IES circles is observed 5 to 10 h following the maximal detection of initiating DSBs (Fig. 1 and 3). However, 70% of the known IESs are shorter than 80 bp, which is hardly compatible with the formation of double-stranded circles. Therefore, IES circles may be only secondary excision products. Indeed, previous Southern blot analysis of genomic DNA from autogamous cells provided evidence that for IESs larger than 200 bp, molecules with the size expected for linear IESs are detected at early stages of macronuclear development (2, 10). Close examination of the blot shown in Fig. 1B indicates that for IES 51A6649, release of the putative linear excised form and IES end cleavage occur within the same time window. Therefore, although a second and later pathway of direct circle excision may not be ruled out definitively, the primary products of excision could be linear molecules carrying 4-base 5′ overhangs (Fig. 7B). They may then be degraded or converted into more stable circles through the intramolecular alignment of their 5′ protruding ends within a circular junction intermediate similar to the one proposed for the healing of chromosomal junctions. According to this model, only the $3'OH$ and $5'PO_4$ groups detected 1 nt 5′ to the TA on its macronuclear side would be generated by an initial phosphodiester bond cleavage. Following this initial step, the free $3'OH$ and $5'PO_4$ groups observed 5′ to the T residue would be produced by two distinct events: gap filling within the macronuclear junction intermediate would create the corresponding 3′ end, while the 5′ end would result from processing of the 5′ overhangs within the circular IES junction intermediate. The lower efficiency of 5′ processing at IES ends relative to macronucleus-destined ends (Fig. 5A and B) suggests that circle formation is less efficient than chromosome end alignment, perhaps because of structural limitations for intramolecular end joining on such short molecules.

***trans*-Acting factors required for DNA cleavage and DSB repair.** We can anticipate that two types of enzymatic activities should be present during macronuclear development in *Paramecium*, to perform the staggered double-strand cleavage specifically at IES boundaries and subsequently join the broken chromosome ends.

A statistical analysis of the macronucleus-destined sequences flanking the ends of 78 IESs from *P. aurelia* (10) leads to identification of the preferred sequence $5'\text{-}T_{52}G_{30}G_{30}\text{-}3'$

(where the numbers represent the observed percent occurrence of each nucleotide) for the three positions adjacent to the conserved 5′-TA-3′ on the macronuclear side, while the expected frequencies for T and G residues are 35 and 15%, respectively, within the flanking macronuclear DNA strand located 5′ to the TA. The overrepresentation of these three nucleotides suggests that flanking residues contribute to the definition of the IES cleavage site, in addition to the TA and the internal consensus sequence of their ends. The nucleotide sequence, however, is probably not the sole determinant for targeting the cleavage at IES boundaries: IES excision in the developing anlagen is, indeed, epigenetically controlled by homologous sequences present in the parental macronucleus (7, 8). Likewise, epigenetic control of excision was found in *Tetrahymena* (3). Another common feature between *Paramecium* and *Tetrahymena* IESs is the strikingly similar geometry of the initiating DSBs, which carry 4-base 5′ overhangs. Therefore, in spite of the different sequences of IES boundaries in the two ciliates, related activities may participate in the recognition and initial cleavage of the ends.

Several endonuclease activities may catalyze the formation of DSBs (4, 11). The first type of candidate enzymes could be transposase-related proteins, which produce only DNA intermediates. It was previously proposed for "TA" IESs in other ciliates that the excising endonuclease could be the transposase encoded by an active copy of Tc/mariner-like transposons present in the germ -line genome (17). However, studies of *Euplotes* indicate that the expression level of their transposase-encoding ORF is too low during macronuclear development to mediate the massive excision of tens of thousands of IESs (14). There remains the possibility that a transposase activity has been recruited by the cell to initiate IES excision. It should be noted that the initial cleavage catalyzed by most transposases is the nicking of a single strand at either or both ends of the mobile sequence, while various strategies have been adopted for second-strand cleavage (32): nucleophilic attack of the opposite strand can generate hairpin structures which are resolved subsequently [Tn*5*, IS*10*, or V(D)J recombination]; alternatively, a second endonuclease activity may be involved (Tn *7*). Enzymes related to site-specific recombinases or topoisomerases could also be involved in IES end cleavage. These proteins generate covalent protein-DNA intermediates, which would not allow the simultaneous liberation of 3′OH and 5′PO_4 groups at a cleaved phosphodiester bond. However, as was proposed for Spo11, a topoisomerase-like protein of yeast involved in meiotic recombination (15), hydrolysis of the protein-DNA bond could release free 5′PO_4 and 3′OH groups on the cleaved DNA. The experimental conditions used in our study (DNA extraction procedure, asynchronous cultures) do not allow us to define the transient early intermediate steps (putative single strand cleavages, covalent DNA-protein complexes, DNA hairpins, etc.) that lead to the DSBs analyzed here. More work is clearly needed, therefore, to identify the molecular details of the reaction and the enzyme(s) involved in IES excision.

The present study provides evidence that macronuclear junction closure after IES excision in *Paramecium* involves the 5′ processing of DSBs. This may result from the fact that excision is initiated by two DSBs, one at each boundary, and from the observed precise joining of broken chromosome ends, in spite of the existence of only partial complementarity between their 4-base overhangs. During the excision of *Tetrahymena* IESs, no DSB processing has been reported. Instead, it was proposed that a single initiating DSB is introduced at one IES boundary and that closure of the chromosomal junction is achieved by the resolution of a branched junction intermediate formed by the direct strand transfer of the first unprocessed macronucleus-destined broken end to the second excision boundary (28). Therefore, junction repair in *Paramecium* would be the first evidence in ciliates for the participation of an end-joining mechanism in IES excision.

ACKNOWLEDGMENTS

We thank Eric Meyer for his constant support throughout the course of this work. We are extremely grateful to Jim Forney and Erika Snodderley for communicating the sequence of IES 51A-4814 prior to publication. We thank Jérôme Chal and Carole Escartin for their participation in the optimization of LMPCR assays, and we thank Edouard Bray for his help with the design of our Web page. Many thanks to Tom Doak and all members of E. Meyer's laboratory for stimulating discussions and to Sandra Duharcourt, Anne Le Mouël, Sophie Malinsky, E. Meyer, and Linda Sperling for critical reading of the manuscript.

This work was supported by the Association pour la Recherche sur le Cancer (grant 5733), the Centre National de la Recherche Scientifique (Soutien aux jeunes équipes), and the Comité de Paris de la Ligue Nationale contre le Cancer (grant 75/01-RS/73). A. Gratias was the recipient of a doctoral fellowship from the French Ministère de la Recherche and is currently supported by the Association pour la Recherche sur le Cancer.

REFERENCES

1. **Berger, J. D.** 1973. Nuclear differentiation and nucleic acid synthesis in well-fed exconjugants of *Paramecium aurelia.* Chromosoma **42:**247–268.
2. **Bétermier, M., S. Duharcourt, H. Seitz, and E. Meyer.** 2000. Timing of developmentally programmed excision and circularization of *Paramecium* internal eliminated sequences. Mol. Cell. Biol. **20:**1553–1561.
3. **Chalker, D. L., and M. C. Yao.** 1996. Non-Mendelian, heritable blocks to DNA rearrangement are induced by loading the somatic nucleus of *Tetrahymena thermophila* with germ line-limited DNA. Mol. Cell. Biol. **16:**3658–3667.
4. **Champoux, J. J.** 2001. DNA topoisomerases: structure, function, and mechanism. Annu. Rev. Biochem. **70:**369–413.
5. **Craig, N. L., R. Craigie, M. Gellert, and A. M. Lambowitz.** 2002. Mobile DNA II. ASM Press, Washington, D.C.
6. **Dawson, A., and D. J. Finnegan.** 2003. Excision of the *Drosophila* mariner transposon Mos1. Comparison with bacterial transposition and V(D)J recombination. Mol. Cell **11:**225–235.
7. **Duharcourt, S., A. Butler, and E. Meyer.** 1995. Epigenetic self-regulation of developmental excision of an internal eliminated sequence in *Paramecium tetraurelia.* Genes Dev. **9:**2065–2077.
8. **Duharcourt, S., A. M. Keller, and E. Meyer.** 1998. Homology-dependent maternal inhibition of developmental excision of internal eliminated sequences in *Paramecium tetraurelia.* Mol. Cell. Biol. **18:**7075–7085.
9. **Garrity, P. A., and B. J. Wold.** 1992. Effects of different DNA polymerases in ligation-mediated PCR: enhanced genomic sequencing and *in vivo* footprinting. Proc. Natl. Acad. Sci. USA **89:**1021–1025.
10. **Gratias, A., and M. Bétermier.** 2001. Developmentally programmed excision of internal DNA sequences in *Paramecium aurelia.* Biochimie **83:**1009–1022.
11. **Hallet, B., and D. J. Sherratt.** 1997. Transposition and site-specific recombination: adapting DNA cut-and-paste mechanisms to a variety of genetic rearrangements. FEMS Microbiol. Rev. **21:**157–178.
12. **Jacobs, M. E., and L. A. Klobutcher.** 1996. The long and the short of developmental DNA deletion in *Euplotes crassus.* J. Eukaryot. Microbiol. **43:**442–452.
13. **Jahn, C. L., and L. A. Klobutcher.** 2002. Genome remodeling in ciliated protozoa. Annu. Rev. Microbiol. **56:**489–520.
14. **Jaraczewski, J. W., J. S. Frels, and C. L. Jahn.** 1994. Developmentally regulated, low abundance Tec element transcripts in *Euplotes crassus*—implications for DNA elimination and transposition. Nucleic Acids Res. **22:**4535–4542.
15. **Keeney, S., C. N. Giroux, and N. Kleckner.** 1997. Meiosis-specific DNA double-strand breaks are catalyzed by Spo11, a member of a widely conserved protein family. Cell **88:**375–384.

16. **Klobutcher, L. A., and G. Herrick.** 1995. Consensus inverted terminal repeat sequence of *Paramecium* IESs: resemblance to termini of Tc1-related and *Euplotes* Tec transposons. Nucleic Acids Res. **23:**2006–2013.
17. **Klobutcher, L. A., and G. Herrick.** 1997. Developmental genome reorganization in ciliated protozoa: the transposon link. Prog. Nucleic Acid Res. Mol. Biol. **56:**1–62.
18. **Klobutcher, L. A., L. R. Turner, and J. LaPlante.** 1993. Circular forms of developmentally excised DNA in *Euplotes crassus* have a heteroduplex junction. Genes Dev. **7:**84–94.
19. **Lampe, D. J., M. E. Churchill, and H. M. Robertson.** 1996. A purified mariner transposase is sufficient to mediate transposition *in vitro.* EMBO J. **15:**5470–5479.
20. **Lampe, D. J., M. E. Churchill, and H. M. Robertson.** 1997. A purified mariner transposase is sufficient to mediate transposition *in vitro.* Erratum. EMBO J. **16:**4153.
21. **Mayer, K. M., and J. D. Forney.** 1999. A mutation in the flanking 5′-TA-3′ dinucleotide prevents excision of an internal eliminated sequence from the *Paramecium tetraurelia* genome. Genetics **151:**597–604.
22. **Meyer, E., and O. Garnier.** 2002. Non-Mendelian inheritance and homology-dependent effects in ciliates. Adv. Genet. **46:**305–337.
23. **Meyer, E., and A. M. Keller.** 1996. A mendelian mutation affecting mating-type determination also affects developmental genomic rearrangements in *Paramecium tetraurelia.* Genetics **143:**191–202.
24. **Mueller, P. R., and B. Wold.** 1989. *In vivo* footprinting of a muscle specific enhancer by ligation-mediated PCR. Science **246:**780–786.
25. **Preer, L. B., G. Hamilton, and J. R. Preer.** 1992. Micronuclear DNA from *Paramecium tetraurelia*: serotype 51 *A* gene has internally eliminated sequences. J. Protozool. **39:**678–682.
26. **Sambrook, J., and D. W. Russell.** 2001. Molecular cloning: a laboratory manual, 3rd ed. Cold Spring Harbor Laboratory Press, Cold Spring Harbor, N.Y.
27. **Saveliev, S. V., and M. M. Cox.** 1996. Developmentally programmed DNA deletion in *Tetrahymena thermophila* by a transposition-like reaction pathway. EMBO J. **15:**2858–2869.
28. **Saveliev, S. V., and M. M. Cox.** 2001. Product analysis illuminates the final steps of IES deletion in *Tetrahymena thermophila.* EMBO J. **20:**3251–3261.
29. **Saveliev, S. V., and M. M. Cox.** 1995. Transient DNA breaks associated with programmed genomic deletion events in conjugating cells of *Tetrahymena thermophila.* Genes Dev. **9:**248–255.
30. **Sonneborn, T. M.** 1970. Methods in *Paramecium* research. Methods Cell Physiol. **4:**241–339.
31. **Sonneborn, T. M.** 1974. *Paramecium aurelia*, p. 469–594. *In* R. C. King (ed.), Handbook of genetics: plants, plant viruses and protists, vol. 2. Plenum Press, New York, N.Y.
32. **Turlan, C., and M. Chandler.** 2000. Playing second fiddle: second-strand processing and liberation of transposable elements from donor DNA. Trends Microbiol. **8:**268–274.
33. **Williams, K., T. G. Doak, and G. Herrick.** 1993. Developmental precise excision of *Oxytricha trifallax* telomere-bearing elements and formation of circles closed by a copy of the flanking target duplication. EMBO J. **12:**4593–4601.
34. **Yao, M. C., S. Duharcourt, and D. L. Chalker.** 2002. Genome-wide rearrangements of DNA in ciliates, p. 730–758. *In* N. L. Craig, R. Craigie, M. Gellert, and A. M. Lambowitz (ed.), Mobile DNA II. American Society for Microbiology, Washington, D.C.